HHS Public Access

Author manuscript

Science. Author manuscript; available in PMC 2018 November 29.

Published in final edited form as:

Science. 2018 August 10; 361(6402): 607–612. doi:10.1126/science.aah4065.

Apoptosis propagates through the cytoplasm as trigger waves

X. Cheng[1] and **J. E. Ferrell Jr.**[1,2]

[1]Dept. of Chemical and Systems Biology, Stanford University School of Medicine, Stanford CA 94305-5174

[2]Dept. of Biochemistry, Stanford University School of Medicine, Stanford CA 94305-5307

Abstract

Apoptosis is an evolutionarily conserved form of programmed cell death critical for development and tissue homeostasis in animals. There are several positive feedback loops in the apoptotic control network, which could allow apoptosis to spread through the cytoplasm in self-regenerating trigger waves. We tested this possibility in cell-free *Xenopus laevis* egg extracts, and observed apoptotic trigger waves with speeds of ~30 μm/min. Fractionation and inhibitor studies implicated multiple feedback loops in generating the waves. Apoptotic oocytes and eggs exhibited surface waves with speeds of ~30 μm/min, which were tightly correlated with caspase activation. Thus apoptosis spreads through trigger waves in both extracts and intact cells. Our findings emphasize the importance of trigger waves in cell signaling, allowing diverse all-or-none decisions to propagate over large distances without decreasing in speed or amplitude.

One Sentence Summary:

Apoptosis propagates through cytoplasm as self-regenerating trigger waves, which spread without slowing down or petering out.

Xenopus laevis eggs are large cells, ~1.2 mm in diameter, that are naturally arrested in metaphase of meiosis II. The eggs ultimately adopt one of two fates: either they become fertilized and enter the embryonic cell cycle, or they fail to become fertilized and die, usually through apoptosis. Apoptosis is a relatively non-perturbing form of cell death, and may allow the frog to resorb old oocytes and to clean up any eggs retained in the frog's body without provoking an inflammatory response (1). The powerful biochemical approaches provided by the *Xenopus* system have made *Xenopus* eggs and extracts useful model systems for the study of apoptosis (2, 3).

*Corresponding author. james.ferrell@stanford.edu.

Author contributions: XC and JEF jointly designed the studies, carried out the computations, made the figures, and wrote the paper. XC carried out the experiments.

Supplemental Materials
Materials and Methods
Figures S1-S9
Movies S1-S10

Competing interests: None declared.

Data and materials availability: All data needed to evaluate the conclusions in the paper are present in the paper or the Supplementary Materials.

The unusual size of the *Xenopus* egg raises the question of how an all-or-none, global process like apoptosis spreads through the cell. One possibility is that apoptosis spreads through the egg by random walk diffusion, ultimately taking over all of the cytoplasm. A second possibility is suggested by the fact that the regulatory network that controls apoptosis contains multiple positive and double-negative feedback loops (Fig. 1A). These loops could allow apoptosis to propagate through self-regenerating trigger waves. Trigger waves are propagating fronts of chemical activity that maintain a constant speed and amplitude over large distances. They can arise when bistable biochemical reactions are subject to diffusion, or, more generally, when something akin to bistability (e.g bistability, excitability, or relaxation oscillations) is combined with a spatial coupling mechanism (e.g. diffusion or cell-cell communication) (4–6). Familiar examples include action potentials, calcium waves, and the spread of a fire through a field, a favorable allele through a population, or a meme through the internet. Trigger waves are an important general mechanism for long-range biological communication, and apoptotic trigger waves could allow death signals to spread rapidly, and without diminishing in amplitude, even through a cell as large as a frog egg.

To distinguish between diffusive spread and trigger waves in the propagation of apoptotic signals, we used undiluted cell-free extracts from *Xenopus* eggs (7). Such extracts can be placed in long (several millimeters) tubes and imaged by video microscopy (8, 9). Over millimeter distances, the distinction between diffusive spread of apoptosis, which would slow down with increasing distance, and trigger waves, which maintain a constant speed and amplitude, should be readily apparent.

We incubated one portion of a cycloheximide-treated interphase cytoplasmic extract with horse cytochrome *c* (2.4 μM) and verified that caspase-3 and/or caspase-7, executioner caspases (10) that share similar peptide sequence specificity, became activated (figure S1). A 10-kD Texas Red-conjugated dextran was added to the apoptotic extract as a diffusion marker, and the extract was pipetted into a large (560-μm inner diameter) Teflon reservoir. We then took a second portion of the interphase extract, with added sperm chromatin plus a chimeric protein consisting of glutathione-S-transferase, green fluorescent protein, and a nuclear localization sequence (GST-GFP-NLS) but no cytochrome *c*, and introduced it into a thin (150-μm inner diameter) Teflon tube. The nuclei act as an easily-assessed indicator of apoptosis: in non-apoptotic extracts, GST-GFP-NLS concentrates in the nuclei that form from the sperm chromatin, whereas in an apoptotic extract, caspases attack components of the nuclear pore (11) and allow the GST-GFP-NLS to leak out and disperse. The tube containing this naive extract was gently inserted a short distance into the reservoir containing the apoptotic extract, and the two tubes were placed under mineral oil (Fig. 1B). We used time-lapse fluorescence microscopy to determine whether apoptosis spread up the thin tube in a diffusive fashion, with propagation slowing as apoptosis proceeded, or at a constant velocity as expected for trigger waves.

As shown in movie S1 and Fig. 1, B and C, apoptosis progressed up the thin tube at a constant speed of 27 μm/min over a distance of several millimeters. In five independent experiments, apoptosis always propagated linearly, without showing any signs of slowing down or petering out, and the average speed was 29 ± 2 μm/min (mean ± S.D.). In contrast,

the 10-kD dye spread only a few hundred microns (Fig. 1B), implying that neither simple diffusion nor any unintended mixing could account for the spread of apoptosis.

If the apoptotic signals are indeed propagated by trigger waves, one prediction is that the waves should be self-sustaining; that is, once the activity is established in the thin tube, continued contact with the reservoir of apoptotic extract would not be required. We tested this possibility by inserting the thin tube into the apoptotic reservoir for 20 min, and then removing it and monitoring apoptosis. The apoptotic activity propagated from the induction terminus to the distal terminus, at a constant speed of 32 μm/min, consistent with a self-sustaining process (figure S2). This procedure was used for all subsequent experiments, because it provided more reliable focusing for the imaging and allowed more tubes to be imaged per experiment.

A second way of detecting apoptosis is with the fluorogenic caspase substrate Z-Asp-Glu-Val-Asp-rhodamine 110 (Z-DEVD-R110) (12). This probe is a rhodamine derivative (R110) with two four-amino acid (DEVD) peptides linked to the fluorophore. It is non-fluorescent when the DEVD-fluorophore bonds are intact, but becomes strongly fluorescent once they are hydrolyzed by caspase-3 or −7. We added the probe (2 μM) to an extract and initiated apoptosis as before. Fluorescence spread up the tube at a constant speed (in this experiment, 33 μm/min). In eight experiments, the average speed was 30 ± 3 μm/min (mean ± S.D.) (movie S2, Fig. 1D). We also added sperm chromatin and GST-mCherry-NLS as well as Z-DEVD-R110 to compare the propagation of the caspase activity wave to the disappearance of the reconstituted nuclei. In this experiment, the disappearance of the nuclei lagged 40 min behind the front of Z-DEVD-R110 fluorescence (Fig. 1E); in four independent experiments the lag was 35 ± 5 min (mean ± S.D.). The speeds of the Z-DEVD-R110 and GST-mCherry-NLS waves—the slopes of the dashed white lines—were indistinguishable (Fig. 1E).

We sought to understand the mechanistic basis for the trigger waves. The apoptotic control system includes multiple positive feedback loops (Fig. 1A). One positive feedback circuit involves only cytosolic proteins, including caspases-3, −7, and −9, and XIAP (designated “caspase loop” in Fig. 1A). Another involves the system that regulates the Bak and Bax proteins (the “BH3 protein loop” in Fig. 1A), which, when activated, bring about mitochondrial outer membrane permeabilization (MOMP). One long loop, in which cytosolic cytochrome *c* stimulates caspase-3 and −7 activation and caspase activation stimulates cytochrome *c* release (the “MOMP/caspase/BH3 protein loop”) connects the two shorter loops (Fig. 1A). We tested whether the cytosolic components could support trigger waves in the absence of mitochondria, and whether the mitochondrial components could support trigger waves in the absence of the activation of caspase-3 and caspase-7.

We fractionated a crude cytoplasmic extract (2, 3) (figure S3A) and verified by immunoblotting that the resulting cytosol was largely devoid of mitochondria, as indicated by the absence of a mitochondrial marker protein, the voltage-dependent anion channel (VDAC) (figure S3B). Horse cytochrome *c* (2.4 μM) was added to this cytosolic fraction, and the activity of caspase-3 and/or −7 was assessed by the chromogenic caspase assay. In agreement with previous reports (3, 13), the caspases were briskly activated (Fig. 2A). Thus

mitochondria are not essential for cytochrome *c*-induced activation of executioner caspases in *Xenopus* extracts.

We tested whether the cytosolic extract could support apoptotic trigger waves. Because nuclei cannot be reconstituted in cytosolic extracts, we used the fluorogenic Z-DEVD-R110 probe for this experiment. The fluorescence spread up the tube in a sub-linear fashion (movie S3, Fig. 2E). To see if this spread was consistent with simple random walk diffusion, we identified points along the propagation front with equal fluorescence intensity (figure S4A and B) and plotted distance squared (x^2) vs. time (figure S4C). The x^2 vs. t relationship was linear for at least an hour (figure S4C), consistent with random walk diffusion. Thus, over this time scale and distance scale, there was no evidence for a trigger wave.

To further test the role of the mitochondria, we added back purified mitochondria to the cytosolic extract at a 3% volume to volume (v/v) ratio, which is approximately physiological [estimated from the volumes we obtained for the various fractions (see figure S3) and the concentrations used by others in reconstitution studies (3)], and again determined whether apoptosis would propagate diffusively or as a trigger wave. As expected, the reconstituted extract activated caspase-3 in response to horse cytochrome *c* (Fig. 2C). Moreover, the reconstitution restored the trigger waves (movie S3 and Fig. 2D). The propagation distance increased linearly with time (Fig. 2D), as it did in crude cytoplasmic extracts (Fig. 1), and had a constant speed of 39 μm/min, somewhat faster than that observed in cytoplasmic extracts. The signal propagated over a long distance (6000 μm) with little loss of amplitude and no loss of speed (Fig. 2D).

Over a distance scale of a millimeter or so it is easy to distinguish a ~30 μm/min trigger wave from diffusive spread of even a rapidly-diffusing small molecule like R110. However, by the end of the experiment shown in Fig. 1B, the speed of the caspase-3 wave had fallen only to ~15 μm/min; a trigger wave any slower than that would be outpaced by diffusion over the same distance. Thus to determine whether trigger waves were abolished or only slowed in cytosolic extracts, we made use of longer tubes (up to 3 cm) and longer time courses (up to 24 h). Display of R110 fluorescence on a pseudocolor heat map scale to made it easier to distinguish the wave front at both early times and late times (Fig. 2E). As was the case in Fig. 2B, the speed of the wave front fell during the first ~120 min, consistent with diffusive propagation, but once the speed reached ~14 μm/min it remained constant for many hours (Fig. 2E). This suggests that purified cytosol is capable of generating apoptotic trigger waves, albeit with a substantially slower speed than that seen in cytoplasm or in cytosol supplemented with mitochondria.

Trigger wave speeds were measured in eight independent experiments using various concentrations of mitochondria (Fig. 2F). From curve fitting, the trigger wave speed was half maximal at a mitochondrial concentration of 1.3 ± 0.6% (mean ± S.E.), which is estimated to be ~40% of the physiological mitochondrial concentration in *Xenopus* eggs. Thus an average concentration of mitochondria is sufficient to generate apoptotic trigger waves of near-maximal speed, and the wave speed would be expected to drop in mitochondrion-poor regions of the cytoplasm.

Apoptosis almost always initiated first at the end of the tube that was dipped in the apoptotic extract (Figs. 1 and 2 and figure S2). However, in experiments with either cytoplasmic extracts or reconstituted extracts, more than half of the time (12/22 and 21/37 tubes, respectively) a second spontaneous apoptotic wave emerged elsewhere in the tube (movie S4 and figure S5A). The velocities of the induced and spontaneous trigger waves were indistinguishable (44 μm/min in the example shown in figure S5A), indicating that they probably represent the same basic phenomenon. Usually the entire tube of extract became apoptotic, as assessed by the Z-DEVD-R110 probe, after 2 hours of incubation (figure S5) and invariably by 4 hours. This global activation of caspase-3 and −7 did not occur in cytosolic extracts (which allowed the extended time course experiment shown in Fig. 2E).

The fact that the wave speed depends upon the concentration of mitochondria implies that the BH3-domain proteins that regulate MOMP may function in generating the trigger waves (Fig. 1A). To further test this possibility, we added recombinant GST-Bcl-2 protein to cytoplasmic extracts to see whether trigger waves were affected. Bcl-2 is a stoichiometric inhibitor of the pro-apoptotic tBid protein and of the pore-forming Bak and Bax proteins, and so the expectation was that GST-Bcl-2 would slow the trigger waves. Adding GST-Bcl-2 decreased the wave speed (Fig. 3A and B, movie S5). The maximum effect [at 400 nM added GST-Bcl-2, which compares to the estimated endogenous Bcl-2 concentration of approximately 140 nM (14)] was a reduction of the speed to about 13 μm/min, the speed seen in purified cytosol. Added GST-Bcl-2 had no effect on the trigger wave speed in cytosolic extracts (Fig. 3C and D), which emphasizes that the waves seen in purified cytosol are probably not caused by contaminating mitochondria. GST-Bcl-2 decreased the trigger wave speed in reconstituted (cytosol + mitochondria) extracts (Fig. 3E and F), just as it did in cytoplasmic extracts.

If the MOMP-caspase-BH3 protein loop contributed to the generation of trigger waves, inhibition of the executioner caspases would be expected to slow or block the waves (Fig. 1A). To test this, we added caspase-3 and −7 inhibitor N-acetyl-Asp-Glu-Val-Asp-aldehyde (Ac-DEVD-CHO) to the reconstituted extracts. Because high concentrations of the inhibitor make it difficult to follow trigger waves with the fluorogenic caspase substrate Z-DEVD-R110, we used an additional probe, tetramethylrhodamine ethyl ester (TMRE), a red fluorescent dye that responds to changes in mitochondrial membrane potential. Non-apoptotic mitochondria accumulate TMRE in their matrices. During apoptosis, the matrix loses TMRE at approximately the time of cytochrome *c* release (15, 16), even in the presence of caspase inhibitors (17). We tested TMRE as a reporter of trigger waves by adding 50 nM TMRE to a reconstituted extract together with Z-DEVD-R110, and looked for evidence of trigger waves in both fluorescence channels. A wave of TMRE loss (and therefore depolarization of mitochondria) could be detected (Figs. 3G and H). The TMRE wave propagated at the same speed as the caspase trigger wave reported by Z-DEVD-R110 in the same tube (38 μm/min).

We tested whether trigger waves still occurred when caspases-3 and −7 were inhibited. When relatively low concentrations of the caspase inhibitor Ac-DEVD-CHO (≤ 1 μM) were used, there was sufficient residual caspase-3 and/or −7 activity to allow both the Z-DEVD-R110 and TMRE reporters to yield data on trigger wave speed. As shown in Fig. 3I-L, figure

S6 and movie S7, Both reporters showed that the wave speed decreased as the inhibitor concentration increased (Fig. 3I through L, figure S6 and movie S7). In the presence of Ac-DEVD-CHO there was a transient increase in TMRE fluorescence at the front of the apoptotic wave, which may result from fluorescence dequenching or transient hyperpolarization, and which made the TMRE waves easier to discern (Fig. 3J and movies S6 and S7). At higher concentrations of Ac-DEVD-CHO, the wave speed could be read out only with the TMRE reporter, and it leveled off at ~15 μm/min (Fig. 3L).

These experiments implicate caspase-3 and/or −7 as well as Bcl-2 in the regulation of the apoptotic trigger waves. The experiments also show that the trigger waves are relatively robust; they are still present, though with reduced speeds, in extracts depleted of mitochondria or treated with maximal doses of GST-Bcl-2 or Ac-DEVD-CHO. However, addition of Ac-DEVD-CHO to cytosolic extracts did completely eliminate trigger waves (figure S7). Thus the cytosolic caspase feedback loop (Fig. 1A) appears to mediate the (slow) apoptotic trigger waves seen in purified cytosolic extracts (Fig. 2E and3C).

To determine whether apoptotic trigger waves occur in intact oocytes and eggs, we imaged oocytes incubated with TMRE or Z-DEVD-R110 and looked for evidence of a wave of fluorescence. However, the opacity of the cells made it difficult to obtain satisfactory imaging data. Nevertheless, we noticed that when oocytes were injected with cytochrome *c*, a wave of changes in the oocyte's natural pigmentation systematically spread from the site of injection to the opposite pole. One particularly striking example of such a wave is shown in montage form in Fig. 4A, as a kymograph in Fig. 4B, and in video form in movie S8; two more subtle examples are shown in movie S9. The surface waves propagated at an apparent speed of ~30 μm/min, similar to the wave speeds seen in apoptotic extracts. Control oocytes injected with Texas Red-dextran in water did not exhibit these surface waves. These findings indicate that apoptotic trigger waves can be produced in oocytes.

To test whether eggs might naturally exhibit a similar surface wave at the end of their lifetimes, we incubated eggs with egg-laying buffer at room temperature, conditions that typically lead to apoptosis by 12 to 24 hours. During this same time period, a surface wave often appeared, originating near the vegetal pole and propagating toward the animal pole, with a typical apparent speed of ~30 μm/min (Fig. 4, C and D and movie S10). This wave was followed by further pigment changes over the next several hours—expansion and then contraction of a white dot at the animal pole (figure S8).

To see whether the surface wave correlated with caspase activation, we harvested and lysed individual eggs just after they underwent such a wave. Every egg that showed a wave had increased caspase activity (Fig. 4, E and F, red points). We also collected eggs during the same time period that had not displayed a wave. None of these eggs had increased caspase activity (Fig. 4, E and F, blue points). These findings support the idea that spontaneous apoptosis typically initiates near the vegetal pole of the egg, and propagates outward and upward from there as a ~30 μm/min trigger wave.

Our results indicate that apoptosis propagates through cytoplasmic *Xenopus laevis* extracts via trigger waves (Fig. 1). The speed of the apoptotic trigger waves depends upon the

concentration of mitochondria, although both cytosolic extracts and GST-Bcl-2-treated cytoplasmic extracts can support slower (~13 μm/min) waves (Figs. 2, 3). Inhibiting caspase-3 and caspase-7 also slowed but did not abolish the waves. These findings show that the phenomenon is highly robust and must involve multiple interlinked bistable systems. We also found evidence for apoptotic waves in cytochrome *c*-injected oocytes and in spontaneously dying eggs, demonstrating that the trigger waves are not an artifact of the extract system.

Imaging studies on mammalian cell lines (18–20), cardiac myotubes (21, 22), and syncytial human trophoblasts (23) have shown that apoptosis typically initiates at a single discrete focus, or a small number of discrete foci, and then spreads rapidly throughout the cell, and in some of these studies the propagation velocities appear to be constant over distances of ~100 μm (18, 19, 21, 22). Although it can be difficult to distinguish between trigger waves and diffusive spread over such short distances, particularly in cells with irregular geometries and inhomogeneous cytoplasm, it seems likely that apoptotic trigger waves occur in many cell types.

There is a close analogy between the mechanisms underpinning the apoptotic trigger waves observed here and calcium waves. The former involves cytochrome *c*-induced release of cytochrome *c* and other apoptotic mediators from the mitochondria, while the latter involves calcium-induced calcium release from the endoplasmic reticulum. The particular proteins involved, storage organelles, and time scales for the two types of trigger waves are all different, but the basic logic is the same.

The ingredients needed for generating a trigger wave are simple; they include a spatial coupling mechanism (like diffusion or intercellular communication) and positive feedback (6). Positive feedback is commonplace in signal transduction, from cell fate induction to biological oscillations to prion formation. And whenever positive feedback is present, there is a possibility of trigger waves, allowing signals to propagate quickly over large distances without diminishing in strength or speed. We suspect there may be many other examples of trigger waves in intra- and intercellular communication.

Supplementary Material

Refer to Web version on PubMed Central for supplementary material.

Acknowledgments:

We thank James Chen's and Dan Jarosz's labs for sharing their microscopes, Hiro Funabiki and Mary Dasso for providing the GST-GFP-NLS construct, and Julia Kamenz and the rest of the Ferrell lab for helpful discussions and comments on the manuscript.

Funding: This work was supported by grants from the National Institutes of Health (R01 GM110564 and P50 GM107615).

References and Notes:

1. Iguchi S, Iwasaki T, Fukami Y, Tokmakov AA, Unlaid Xenopus eggs degrade by apoptosis in the genital tract. BMC Cell Biol. 14, 11 (3 03, 2013). [PubMed: 23452868]

2. Newmeyer DD, Farschon DM, Reed JC, Cell-free apoptosis in Xenopus egg extracts: inhibition by Bcl-2 and requirement for an organelle fraction enriched in mitochondria. Cell 79, 353–364 (1994). [PubMed: 7954801]

3. Deming P, Kornbluth S, Study of apoptosis in vitro using the Xenopus egg extract reconstitution system. Meth. Mol. Biol 322, 379–393 (2006).

4. Tyson JJ, Keener JP, Singular perturbation theory of traveling waves in excitable media (a review). Physica D 32, 327–361 (1988).

5. Winfree AT, Two kinds of wave in an oscillating chemical solution. Faraday Symp. Chem. Soc 9, 38–46 (1974).

6. Gelens L, Anderson GA, Ferrell JE, Jr., Spatial trigger waves: positive feedback gets you a long way. Mol. Biol. Cell 25, 3486–3493 (11 5, 2014). [PubMed: 25368427]

7. Murray AW, Cell cycle extracts. Meth. Cell. Biol 36, 581–605 (1991).

8. Chang JB, Ferrell JE, Jr., Mitotic trigger waves and the spatial coordination of the Xenopus cell cycle. Nature 500, 603–607 (8 29, 2013). [PubMed: 23863935]

9. Chang JB, Ferrell JE, Jr., Robustly cycling Xenopus laevis cell-free extracts in Teflon chambers. Cold Spring Harb. Protoc (2 23, 2018). doi: 10.1101/pdb.prot097212 [Epub ahead of print]

10. Tait SW, Green DR, Mitochondria and cell death: outer membrane permeabilization and beyond. Nature Rev. Mol. Cell Biol 11, 621–632 (9, 2010). [PubMed: 20683470]

11. Ferrando-May E, Nucleocytoplasmic transport in apoptosis. Cell Death Differ. 12, 1263–1276 (10, 2005). [PubMed: 15861192]

12. Liu J et al., Fluorescent molecular probes V: a sensitive caspase-3 substrate for fluorometric assays. Bioorg. Med. Chem. Lett 9, 3231–3236 (11 15, 1999). [PubMed: 10576694]

13. Zou H, Li Y, Liu X, Wang X, An APAF-1.cytochrome c multimeric complex is a functional apoptosome that activates procaspase-9. J. Biol. Chem 274, 11549–11556 (4 23, 1999). [PubMed: 10206961]

14. Wühr M et al., Deep proteomics of the Xenopus laevis egg using an mRNA-derived reference database. Curr. Biol, (6 18, 2014).

15. Goldstein JC, Waterhouse NJ, Juin P, Evan GI, Green DR, The coordinate release of cytochrome c during apoptosis is rapid, complete and kinetically invariant. Nat. Cell. Biol 2, 156–162 (3, 2000). [PubMed: 10707086]

16. Rehm M, Dussmann H, Prehn JH, Real-time single cell analysis of Smac/DIABLO release during apoptosis. J. Cell. Biol 162, 1031–1043 (9 15, 2003). [PubMed: 12975347]

17. Waterhouse NJ et al., Cytochrome c maintains mitochondrial transmembrane potential and ATP generation after outer mitochondrial membrane permeabilization during the apoptotic process. J. Cell. Biol 153, 319–328 (4 16, 2001). [PubMed: 11309413]

18. Lartigue L et al., An intracellular wave of cytochrome c propagates and precedes Bax redistribution during apoptosis. J. Cell. Sci 121, 3515–3523 (11 1, 2008). [PubMed: 18840646]

19. Bhola PD, Mattheyses AL, Simon SM, Spatial and temporal dynamics of mitochondrial membrane permeability waves during apoptosis. Biophys. J 97, 2222–2231 (10 21, 2009). [PubMed: 19843454]

20. Rehm M et al., Dynamics of outer mitochondrial membrane permeabilization during apoptosis. Cell Death Differ. 16, 613–623 (4, 2009). [PubMed: 19136937]

21. Pacher P, Hajnoczky G, Propagation of the apoptotic signal by mitochondrial waves. EMBO J. 20, 4107–4121 (8 1, 2001). [PubMed: 11483514]

22. Garcia-Perez C et al., Bid-induced mitochondrial membrane permeabilization waves propagated by local reactive oxygen species (ROS) signaling. Proc. Natl. Acad. Sci. USA 109, 4497–4502 (3 20, 2012). [PubMed: 22393005]

23. Longtine MS, Barton A, Chen B, Nelson DM, Live-cell imaging shows apoptosis initiates locally and propagates as a wave throughout syncytiotrophoblasts in primary cultures of human placental villous trophoblasts. Placenta 33, 971–976 (12, 2012). [PubMed: 23102999]

24. Cheng EH et al., Conversion of Bcl-2 to a Bax-like death effector by caspases. Science 278, 1966–1968 (12 12, 1997). [PubMed: 9395403]

25. Slee EA, Keogh SA, Martin SJ, Cleavage of BID during cytotoxic drug and UV radiation-induced apoptosis occurs downstream of the point of Bcl-2 action and is catalysed by caspase-3: a potential feedback loop for amplification of apoptosis-associated mitochondrial cytochrome c release. Cell Death Differ. 7, 556–565 (6, 2000). [PubMed: 10822279]

26. Albeck JG, Burke JM, Spencer SL, Lauffenburger DA, Sorger PK, Modeling a snap-action, variable-delay switch controlling extrinsic cell death. PLoS Biol. 6, 2831–2852 (12 2, 2008). [PubMed: 19053173]

27. Legewie S, Bluthgen N, Herzel H, Mathematical modeling identifies inhibitors of apoptosis as mediators of positive feedback and bistability. PLoS Comput. Biol 2, e120 (9 15, 2006). [PubMed: 16978046]

28. Zhang T, Brazhnik P, Tyson JJ, Computational analysis of dynamical responses to the intrinsic pathway of programmed cell death. Biophys. J 97, 415–434 (7 22, 2009). [PubMed: 19619456]

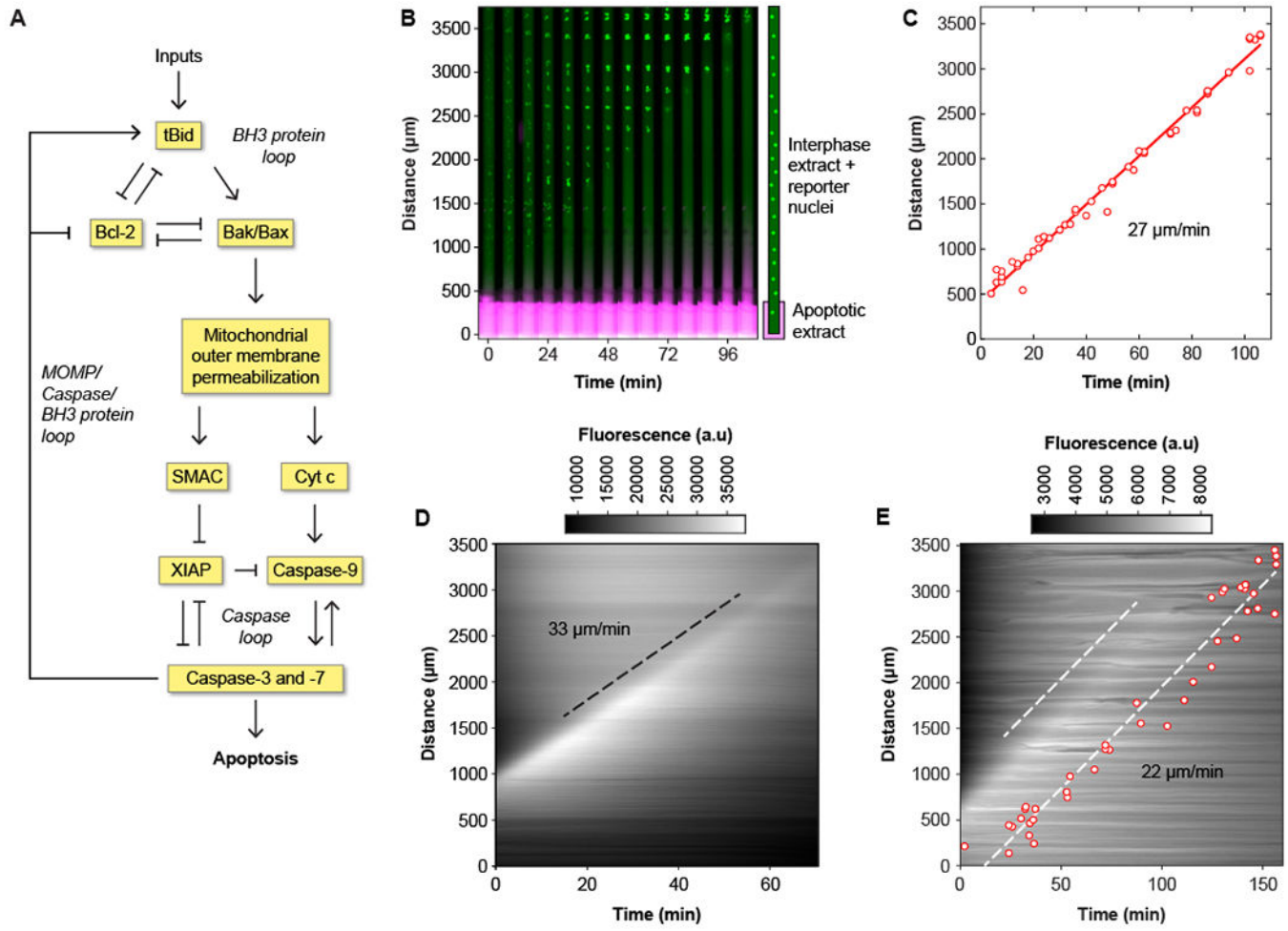

Fig. 1. Apoptosis propagates in interphase-arrested cytoplasmic *Xenopus laevis* egg extracts by trigger waves.

(**A**) The control circuit for apoptosis, adapted from previously published work (24–28). (**B**) Time-lapse montage of GST-GFP-NLS filled nuclei (green) in a cytoplasmic extract in a Teflon tube with its lower end in contact with an apoptotic extract reservoir. The extract in the reservoir is marked with 10-kD dextran-Texas Red dye, shown in magenta. A time-lapse video of this experiment can be found in movie S1. (**C**) Correlation between timing and position of nuclear disappearance for the experiment shown in panel (**B**). The solid red line is a linear least squares fit to the data. The propagation speed (the slope of the fitted line) is 27 µm/min. (**D**) Kymograph showing the spatial propagation of caspase-3 and/or caspase-7 activity (indicated by R110 fluorescence) in a crude cytoplasmic extract. The black dashed line was manually fitted to the fluorescence front, and it yielded a propagation speed of 33 µm/min. (**E**) R110 fluorescence and nuclear disappearance, using GST-mCherry-NLS as a nuclear marker, measured in the same tube. Note that the presence of the nuclei makes the R110 fluorescence less diffuse than it is in panel D. One dashed line is manually fitted to the fluorescence front, and the other is a least-squares fit to the nuclear data. The propagation speed was 22 µm/min for both waves.

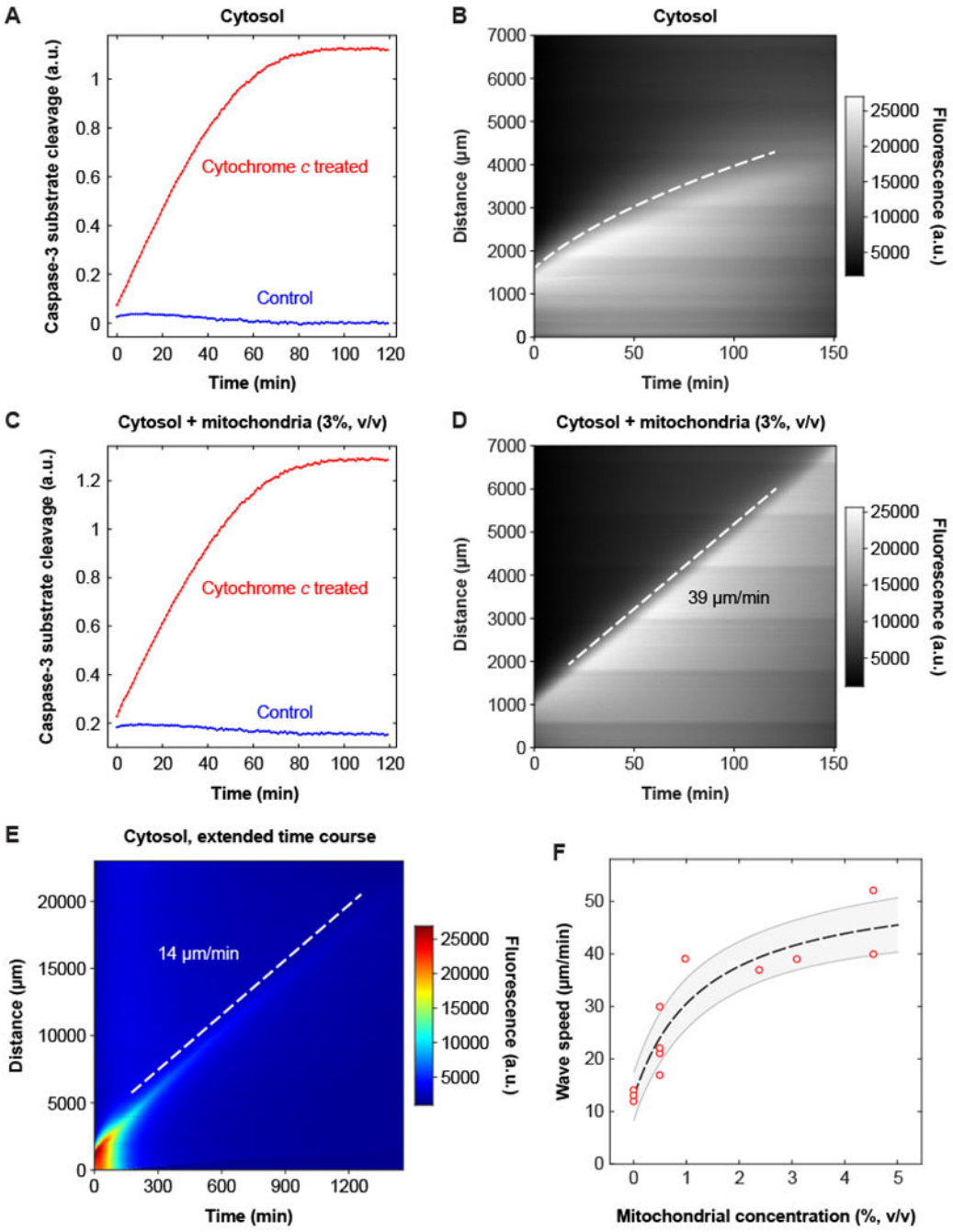

Fig. 2. The speed of the apoptotic trigger wave depends upon the concentration of mitochondria.

(**A**, **B**) Cytosolic extract. Panel A shows activation of caspase-3 and/or caspase-7, by a chromogenic assay, and panel B is a kymograph showing diffusive spread of caspase-3/7 activation, as read out by the Z-DEVD-R110 probe, over this time scale and distance scale. The dashed curve was obtained by defining an equal-fluorescence isocline, replotting the isocline on a distance squared vs. time plot, carrying out a linear least squares fit, and then transforming the fitted line for plotting on the original distance vs. time axes. Further details are provided in figure S4. (**C, D**) Reconstituted extract from the same experiment. Panel C

shows activation of caspase-3 and/or −7 and panel D is a kymograph, here showing trigger wave propagation of caspase activation. (**E**) Slow apoptotic trigger waves detected in cytosolic extracts. This kymograph shows a cytosolic extract incubated for 24 h in a 3 cm tube. R110 fluorescence is displayed here on a heat map scale to allow the shape of the wave front to be appreciated both early and late in the time course. (**F**) Wave speed as a function of mitochondrial concentration. Data are from 18 tubes and 8 independent experiments (there are 9 overlapping data points with 0% mitochondria). The dashed line is a Michaelian dose-response curve given by the equation $y = y_0 + y_{max}\frac{x}{K+x}$; the fitted parameters are y_0 = 13.0±1.4 μm/min, y_{max} = 41.3±6.1 μm/min, and K = 1.3±0.6% (means ± S.E.), and r^2 = 0.98. The grey region is the standard error (68.2% confidence interval) single prediction confidence band calculated with Mathematica 11.1.1.

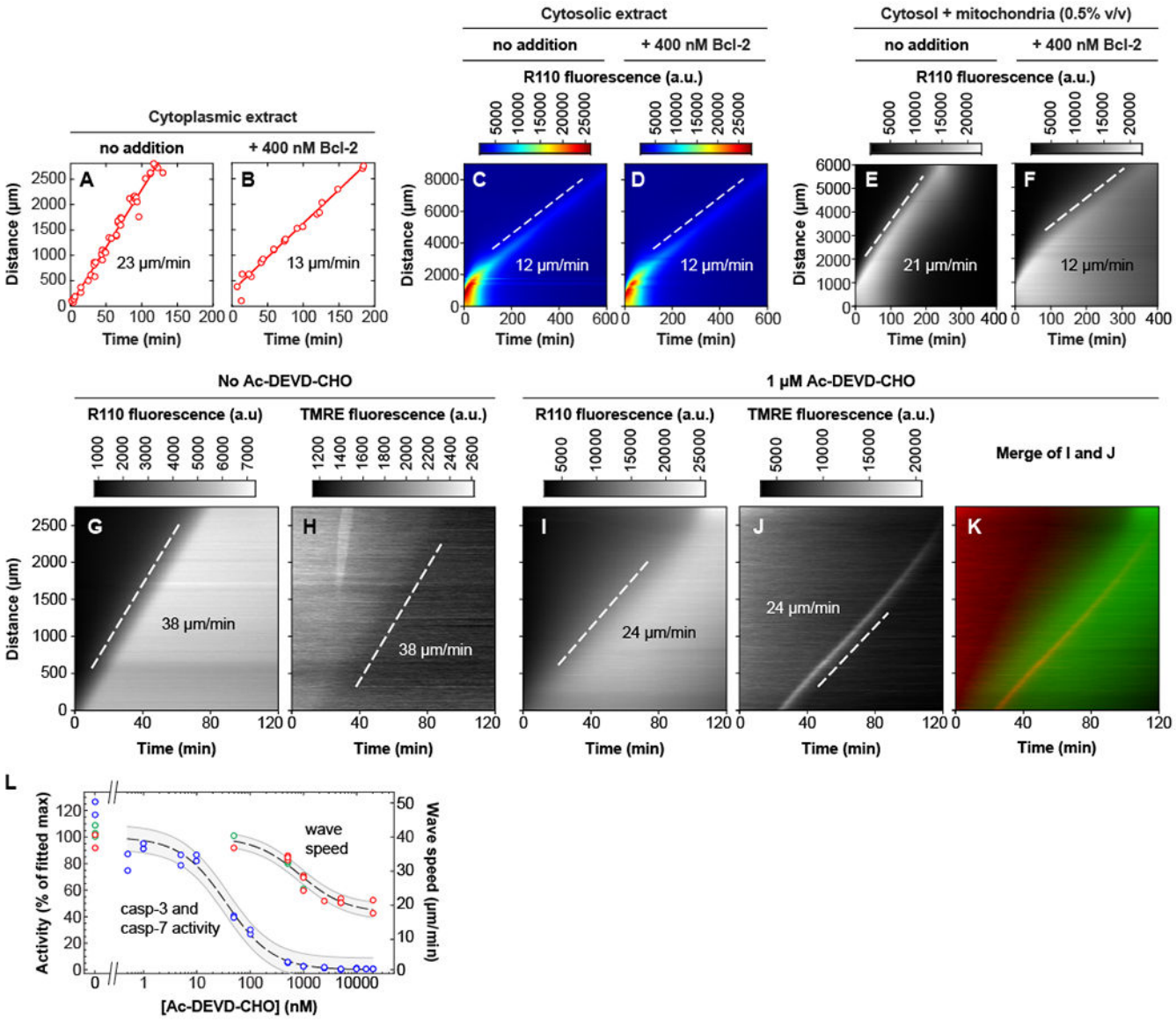

Fig. 3. Both GST-Bcl-2 addition and inhibition of caspase-3 and caspase-7 affect the speed of the trigger waves.

(**A, B**) GST-Bcl-2 reduces the speed of trigger waves in cytoplasmic extracts. Apoptosis was monitored by the disappearance of reporter nuclei containing GST-mCherry-NLS. (**C, D**) GST-Bcl-2 has no effect on the speed of trigger waves in cytosolic extracts. Apoptosis was detected with Z-DEVD-R110, whose fluorescence can be activated by caspase-3 or caspase-7. The pseudocolor heat map scale allows both the initial and final shapes of the wave front to be discerned. (**E, F**) GST-Bcl-2 reduces the speed of trigger waves in extracts reconstituted with cytosol and mitochondria (0.5% v/v). (**G-K**) Inhibition of caspase-3 and −7 slows trigger waves. The reporters were Z-DEVD-R110 and the mitochondrial probe TMRE. (**G, H**) Cytosolic extract reconstituted with mitochondria (2.4% v/v). (**I-K**) A reconstituted extract treated with the caspase inhibitor Ac-DEVD-CHO (1 μM). In experiments with higher concentrations of Ac-DEVD-CHO, a brief (~10 min) period when

the TMRE wave appeared to be parabolic rather than linear was seen (figure S9). (**L**) Inhibition of caspase-3 and −7 activity, and slowing of trigger waves, as a function of Ac-DEVD-CHO concentration in cytosolic extracts reconstituted with mitochondria (2.4% v/v). Blue data points show caspase activities, measured in extracts diluted 1:20. Green data points indicate wave speeds estimated from Z-DEVD-R110 fluorescence, and red points from TMRE fluorescence. The curves are fits to a Michaelian inhibition function, $y = y_0 + (y_{max} - y_0)\frac{K}{K + x}$, where y is the caspase activity or trigger wave speed, x is the Ac-DEVD-CHO concentration, and y_0, y_{max}, and K are parameters determined by fitting the data. For the caspase activity curve, the fitted parameter values were: $y_0 = 0.1 \pm 2.5$; $y_{max} = 100 \pm 3$; and $K = 36 \pm 8$ nM (mean ± S.E.). For the wave speed curve, the fitted parameter values were $y_0 = 17 \pm 1$ μm/min; $y_{max} = 40 \pm 1$ μm/min; and $K = 856 \pm 160$ nM (mean ± S.E.). The shaded regions are the standard error (68.2% confidence interval) single prediction confidence bands calculated with Mathematica 11.1.1.

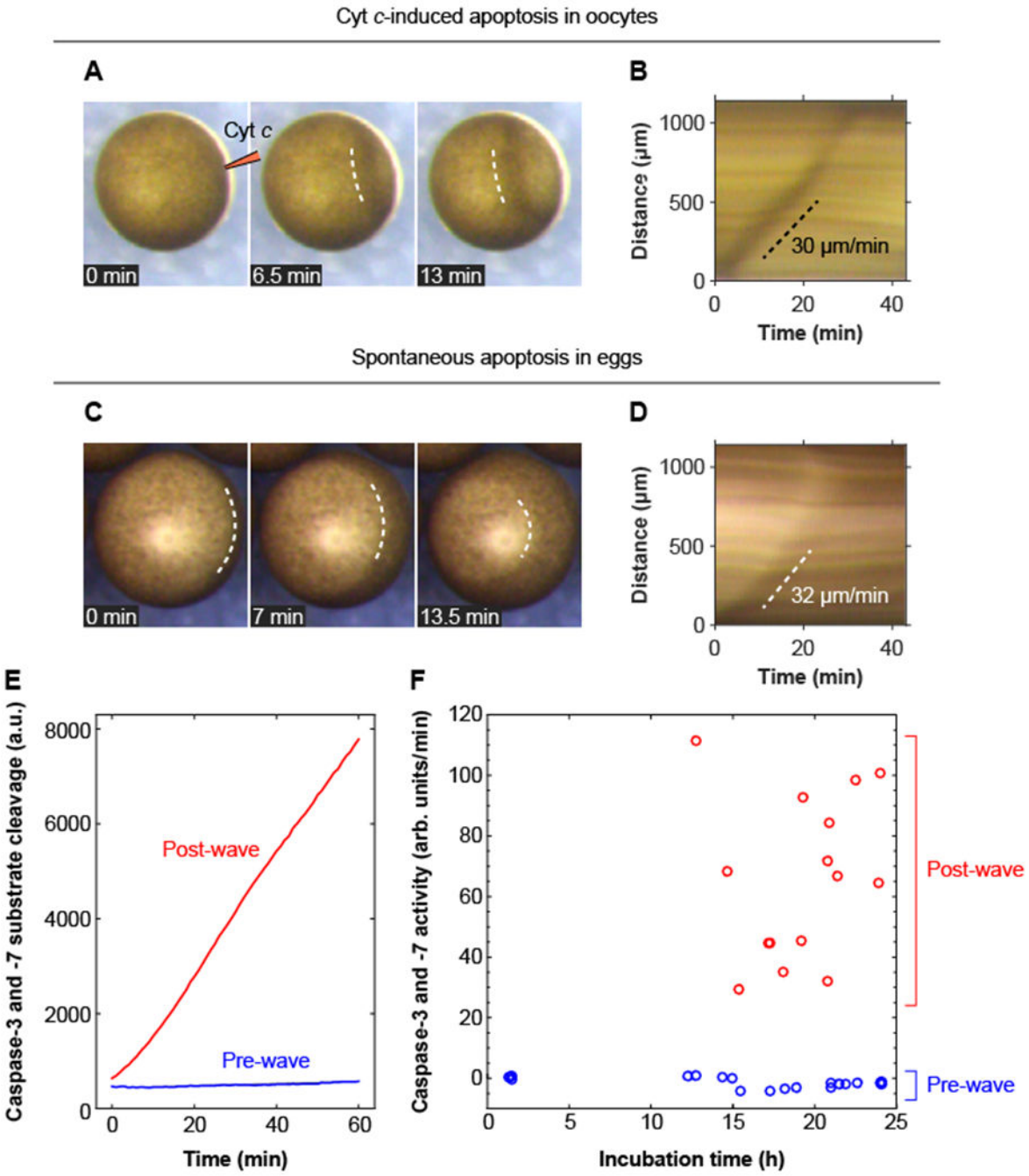

Fig. 4. Apoptotic trigger waves in intact oocytes and eggs.

(**A, B**) Injection of immature Stage VI oocytes with cytochrome *c* (10 nl of 1 mg/ml cytochrome *c*) causes a wave of pigmentation changes to spread from the injection site to the opposite side of the oocyte. Panel A shows one example of this surface wave in montage form; panel B shows the kymograph. Two other examples of these waves are shown in movie S9. (**C, D**) Surface waves occur in spontaneously dying eggs. Panel C shows an example of this wave in montage form, and panel D shows the kymograph. (**E**) Caspase-3 and/or caspase-7 assays for one pre-wave and one post-wave egg. (**F**) Caspase-3 and/or −7

activities for eggs pre- and post-wave. The data are from 19 pre-wave eggs and 15 post-wave eggs.